



# MR Imaging of Osteoid Osteoma: Pearls and Pitfalls

Jerry French, BS,<sup>\*,†</sup> Monica Epelman, MD,<sup>\*,†</sup> Craig M. Johnson, DO,<sup>\*,†</sup>  
Zachary Stinson, MD,<sup>‡</sup> and Arthur B. Meyers, MD<sup>†,§</sup>

Osteoid osteoma (OO) is a benign bone neoplasm consisting of a central prostaglandin-secreting nidus surrounded by a zone of reactive sclerosis. The diagnosis is suspected in children and young adults with longstanding nighttime pain that is relieved by salicylates or nonsteroidal anti-inflammatory drugs. Early studies suggested that computed tomography had a higher sensitivity and specificity in the diagnosis of OO compared to magnetic resonance imaging (MRI). More recent literature suggests MRI done with dynamic postcontrast imaging to be equal to or slightly better at detecting the nidus of OOs, particularly the ones in atypical locations. Being able to evaluate for OO utilizing MRI is important given that the majority of these lesions occur in younger patients, in whom there is greater concern to limit ionizing radiation. Furthermore, patients with atypical OOs often receive an MRI if radiographs are not suggestive of the diagnosis. Therefore, it is important for radiologists to be aware of the imaging features that can help make the diagnosis on MRI.

Semin Ultrasound CT MRI 41:488-497 © 2020 Elsevier Inc. All rights reserved.

## Introduction

Osteoid osteoma (OO) is a term coined by Jaffe in 1935 to describe a series of similar cases of bone lesions that were chronic, sclerosing, and nonsuppurative.<sup>1</sup> OOs are benign, primary bone neoplasms that account for approximately 10% of all biopsied benign bone neoplasms.<sup>2,3</sup> Males develop OO twice as often as females, with individuals between the ages of 10 and 20 being at the greatest risk.<sup>1-3</sup> Nearly any bone in the body is susceptible to developing an OO, however, the diaphysis or metaphysis of the femur or tibia are affected in most cases.<sup>1-3</sup> The next most commonly affected locations are the posterior elements of the vertebrae and bones of the hands and feet.<sup>1,2</sup> Less commonly, OO may be found in bones of the skull and mandible.<sup>1</sup>

OO lesions have a spheroidal nidus that is composed of osteoid and woven bone, embedded within highly vascularized

stroma.<sup>2,4</sup> The sclerosis that surrounds the nidus is composed of dense bone of varying degrees of maturity.<sup>4</sup> The nidus of OO lesions typically measures less than 2 cm in diameter and secretes prostaglandins. This characteristic pathology leads to the hallmark symptom reported by patients with OO – nighttime pain that is ameliorated by salicylates or nonsteroidal anti-inflammatory drugs (NSAIDs), which is present in up to 75% of patients with OO.<sup>5</sup> Though not diagnostic for OO, this combination of symptoms and remedy raises suspicion for OO. The pain relief associated with NSAIDs has been attributed to the inhibition of this prostaglandin production.<sup>6</sup> Prostaglandin levels in the nidus are 100-1000 times that of normal bone and are thought to be important in the perception of pain.<sup>7</sup> Pain is often referred to a nearby joint or may be so distant from the lesion that radiographic examinations can be misdirected. Patients also present with additional complaints specific to the particular location of the OO that may include gait abnormalities, scoliosis, reduced range of motion, and growth disturbances. It is possible that OOs may spontaneously regress over several years with conservative treatment.<sup>8</sup> Unsurprisingly, patients often opt for immediately curative measures such as radiofrequency ablation (RFA) or resection.<sup>8-11</sup>

A successful surgical intervention requires pinpointing the exact location of the nidus on imaging prior to the procedure, as removal of the entire nidus is necessary for cure. Computed tomography (CT) can accomplish this task. However, modern advancements in magnetic resonance imaging

\*University of Central Florida College of Medicine, Orlando, FL.

†Department of Radiology, Nemours Children's Health System/Nemours Children's Hospital, Orlando, FL.

‡Department of Orthopedics, Nemours Children's Health System/Nemours Children's Hospital, Orlando, FL.

§Department of Radiology, Cincinnati Children's Hospital Medical Center, Cincinnati, OH.

Address reprint requests to Arthur B. Meyers, Department of Radiology, Nemours Children's Health System/Nemours Children's Hospital, 13535 Nemours Pkwy, Orlando, FL 32827. E-mail:

[arthur.meyers@cchmc.org](mailto:arthur.meyers@cchmc.org)

(MRI) have allowed for the identification of several useful imaging sequences and novel signs for differentiating OO from potential mimics including osteomyelitis, stress fracture, and other bone neoplasms. Such advancements are clinically important because OO occurs most commonly in younger patients in whom efforts should be made to limit exposure to the ionizing radiation. Furthermore, if the initial radiographic assessment in a child with musculoskeletal pain does not show characteristic findings of an OO, MRI is typically performed as the next step. For these reasons, it is important for radiologists to be able to identify and diagnose OO using MRI. In this review, we will summarize the MR imaging strategies for the evaluation of OO in pediatric patients. In addition, typical and atypical MR imaging features of OO that aid in its differentiation from other lesions are illustrated.

## Classifications

The location of the nidus relative to the surrounding bone tissue layer can be used to separate OOs into 4 distinct classifications.<sup>12</sup> From deep to superficial, the 4 classifications include medullary, endosteal, intracortical, and subperiosteal (Fig. 1). Each of these classes of OO have slight variations in appearance on MRI owing to the interaction of the nidus with the surrounding tissue.

The most common type of OO is intracortical, usually in the diaphysis or metaphysis of long tubular bones. Prominent cortical thickening in the long bones of the lower extremities is common in diaphyseal, intracortical OOs. The characteristic radiographic appearance of an intracortical diaphyseal OO is a small (<2 cm) round or oval lucent nidus located within the cortex at the center of the cortical thickening. However, sometimes extensive cortical thickening can obscure radiographic detection of the nidus. Rarely, central calcifications, corresponding to immature mineralized bone, can be detected within the nidus on radiographs. Very rarely an OO may have more than one nidus.<sup>4</sup>

Medullary, endosteal, subperiosteal, and intra-articular OOs do not have the characteristic imaging appearance as

diaphyseal intracortical OOs. Medullary OOs (also known as cancellous) feature a nidus that is confined to the bone marrow and are often juxta-articular. Lesions in which the nidus is situated along the internal aspect of the cortex are considered endosteal. Endosteal OOs were not included in the original classification system by Edeiken et al. in 1966,<sup>1</sup> but have been included in more recent studies.<sup>12-14</sup> A unique feature of medullary and endosteal OOs is that the nidus may be asymmetrically located, rather than centrally located, within surrounding reactive edema and sclerotic tissue. When the nidus is found on the external aspect of the bony cortex, it is considered subperiosteal. It has been hypothesized that subperiosteal OOs may migrate to intracortical, endosteal, and medullary locations. This is thought to be caused by pressure atrophy and erosion of deep bone layers with concurrent deposition of new bone superficial to the nidus.<sup>12,15</sup>

## MRI and CT for Imaging Evaluation of OO

A number of studies have reported CT to be more sensitive and specific for the evaluation of OO compared to MRI.<sup>16-20</sup> In one of the early studies evaluating OO on MRI versus CT in 1993, Goldman et al. reported 4 cases of OO in the femoral neck for which both CT and MRI were available.<sup>18</sup> In this study the nidi of the OO were not identified prospectively on the MRI exams and therefore the secondary findings of bone marrow edema and reactive synovitis were misinterpreted as being related to other etiologies ranging from malignancy, osteonecrosis, stress fracture to juvenile idiopathic arthritis. A year later in 1994, a study by Assoun et al. reported CT to be more accurate than MRI in detecting the nidus of an OO in 63% of their 19 patients.<sup>16</sup> In the following decade both Davies et al. and Hosalkar et al. published studies reporting the superiority of CT for the evaluation of OO versus MRI, further suggesting that potential for misdiagnosis of OO on MRI.<sup>17,19</sup> In the 2005 study, Hosalkar et al. blinded radiologists to the diagnosis of OO and asked them to classify the lesions on CT and MRI as benign-latent, benign-aggressive, or malignant and to give the most likely diagnosis.<sup>19</sup> In this study, CT classified OO as benign-latent in 81% of cases and benign-aggressive in 18% of cases, while MR classified OO as 19% as benign-latent, 69% as benign-aggressive and 11% as malignant.<sup>19</sup> Additionally, CT diagnosed OO correctly in 67% of cases, whereas MRI made the diagnosis in only 3% of these cases.<sup>19</sup>

In contrast to these studies in 2000, Spouge and Thain, compared the performance of CT relative to MRI for the OO in 10 patients to determine the features of OOs on MR imaging.<sup>14</sup> They concluded that given the superior contrast discrimination of MRI combined with the rapidly evolving MRI technology resulting in higher resolution images, MRI has the potential for improved lesion detection.<sup>14</sup> In 2003, Liu et al. found MRI with dynamic postcontrast images to depict the nidus of an OO with greater conspicuity than nonenhanced MRI and equal to or better conspicuity than with thin-section CT.<sup>21</sup> A later study in 2009 by Zama et al. went



**Figure 1** Classification of OO lesions based on the location of the central nidus (black dots) and of the edema into the surrounding bone (red/orange). From left to right: Normal bone, subperiosteal OO, intracortical OO, endosteal OO and intramedullary OO. Acknowledgement: Medical illustration by Ryan Dickerson, University of Central Florida College of Medicine. (Color version of figure is available online.) OO, Osteoid osteoma.

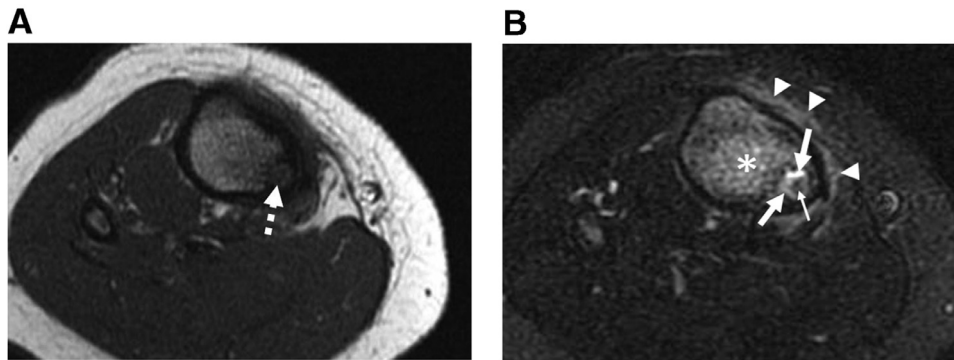


**Figure 2** Two-year-old boy with right leg pain and a pathologically proven OO. Axial (A) T1-weighted and (B) T2-weighted fat saturated MR images show an endosteal OO in the medial aspect of the proximal tibia. The nidus is predominately intermediate to low signal intensity on the T1-weighted image (dashed arrow). On the T2-weighted image the nidus is heterogenous with a “target” appearance with low signal in the most central portion (thin solid arrow) with peripheral increased signal. There is also pronounced edema-like signal within the adjacent medullary cavity (asterisk) and periosteal edema-like signal (arrowheads). OO, Osteoid osteoma

on to evaluate dynamic enhanced MRI versus nonenhanced MRI and CT in the evaluation of OOs in atypical locations.<sup>22</sup> This study is important because as noted above OOs in atypical locations (eg, intra-articular) often do not have a characteristic radiographic appearance. Evaluating the MR and CT findings in 19 patients with pathologically proven OOs these authors found dynamic MRI significantly increased nidus conspicuity compared to nonenhanced MRI and CT. In 31.6% of their cases, nidus conspicuity was higher with dynamic MRI versus CT, leading to a confident diagnosis of OO in 100% of their patients with MRI compared to only 52.6% on with CT. These findings led the authors to conclude that for patients with OO in atypical locations, dynamic MRI increases nidus conspicuity, allowing for more confident diagnosis.<sup>22</sup> The imaging appearance of OO on dynamic postcontrast MRI will be described below. These studies support the idea that contrary to conventional

thought, CT may not be the preferred method of imaging OOs. The use of dynamic enhanced MR sequences is an important part of this change, but other MRI findings and “signs” discussed in the following section have been described that help improve the diagnostic accuracy of OOs on MRI.<sup>23,24</sup>

## MRI Imaging of Osteoid Osteoma

### Standard Sequences

The nidus of an OO is intermediate to low signal intensity on T1-weighted MR sequences (Fig. 2) and has variable signal on T2-weighted sequences depending upon the amount of mineralized matrix within the nidus. Mineralized matrix within the nidus will be low signal intensity on T1- and T2-

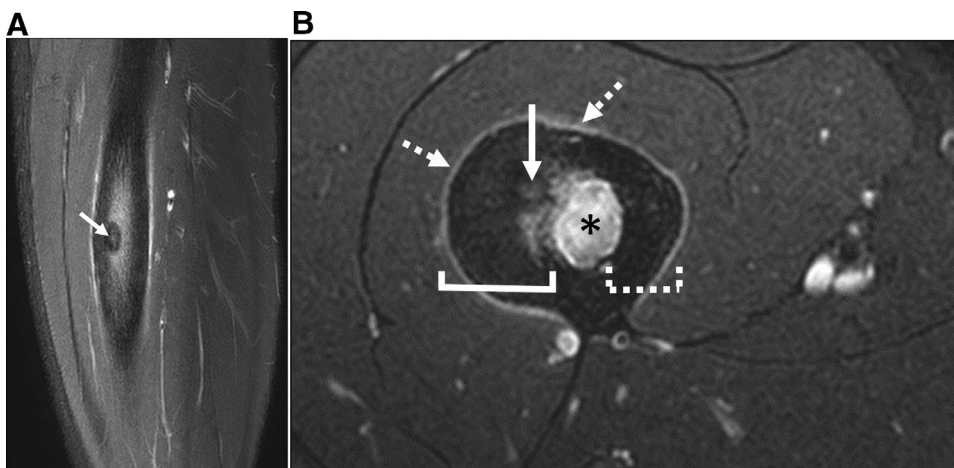


**Figure 3** A 15-year-old boy with right thigh pain that improves with NSAIDs. (A) Coronal and (B) axial T2-weighted fat saturated MRI shows an intracortical OO. The nidus (solid arrow) has increased signal intensity and is located within the anteriomedial cortex of the femur. Note the marked cortical thickening of the medial femoral cortex (solid lines) adjacent to the OO versus the normal lateral cortex (dashed lines). There is also pronounced edema-like signal within the adjacent medullary cavity (asterisk) and mild periosteal edema-like signal (dashed arrow). NSAIDs, nonsteroidal anti-inflammatory drugs; OO, Osteoid osteoma.



weighted sequences. The nonmineralized matrix is typically high signal intensity on T2-weighted sequences (Fig. 3). The nidus can have a “target” appearance on T2-weighted images (Fig. 4) with low signal intensity centrally surrounded by increased signal. The central area of low signal intensity is thought to be secondary to a partially mineralized central portion of matrix, as is sometimes seen on CT (Fig. 4).<sup>25</sup> Intracortical lesions in the diaphysis typically will have cortical thickening surrounding the nidus (Fig. 3), while the other types of OO may have little to no cortical thickening. Edema-like signal within the adjacent bone marrow and periosteal soft tissues is typical (Figs. 2-4).

### Dynamic Contrast Enhanced MRI

An OO nidus contains highly vascularized osteoid tissue and woven bone. It is lined by a layer of bone-forming osteoblasts that produce the above mentioned zone of reactive sclerosis. Conveniently for the radiologist, this vascularized tissue within the nidus can have a characteristic enhancement pattern. In studies evaluating the enhancement pattern of OO on dynamic MRI the majority of lesions will show intense enhancement of the nidus beginning in the arterial phase of enhancement, which is much more pronounced than enhancement in the adjacent bone marrow, with subsequent partial washout by the early venous phase of enhancement.<sup>21,22</sup> This enhancement pattern can be qualitatively appreciated by comparing MR images from the early arterial phase (approximately 30 seconds post injection) with images from the early venous phase of enhancement (approximately 90 seconds post injection) (Fig. 5). The enhancement pattern can also be evaluated quantitatively by drawing regions of interest on the nidus of the OO and obtaining the nidus time–enhancement curves with dedicated software.<sup>22</sup> Various studies have shown early arterial enhancement to be present in 83%-100% of OOs.<sup>13,21,22,26</sup> By using dynamic contrast-enhanced MRI, it is possible to differentiate OO

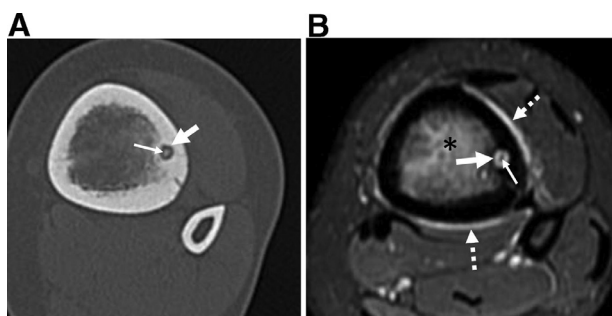


**Figure 4** A 15-year-old girl with left ankle pain. (A) Axial CT shows an endosteal OO in the anteriolateral aspect of the distal left tibia. The nidus is lucent (thick solid arrow) with a small punctate area of with ossified matrix (thin solid arrow). (B) Axial T2-weighted fat saturated MRI shows a “target” appearance of the nidus with high signal peripherally (thick solid arrow) and low signal centrally (thin solid arrow) which corresponds to the mineralized matrix centrally within the nidus on CT. Edema-like signal within the adjacent medullary cavity (asterisk) and periosteal edema-like signal (dashed arrow) are also present. OO, Osteoid osteoma.

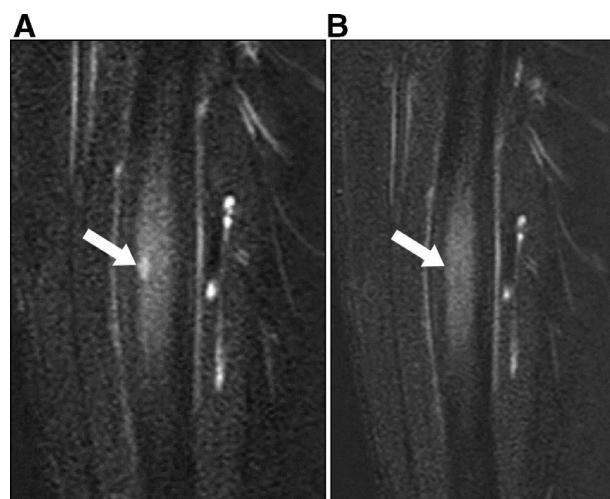


**Figure 5** A 15-year-old boy with right thigh pain that improves with NSAIDs. Postcontrast T1-weighted subtraction images during the early arterial and delayed phases of contrast enhancement. The nidus (arrows) shows avid enhancement on the early arterial phase (A) which is hyperintense to the enhancement in the adjacent bone marrow edema and washes out to become isointense to the adjacent bone marrow edema enhancement on the delayed phase (B). This pattern of enhancement is characteristic of OO. NSAIDs, nonsteroidal anti-inflammatory drugs; OO, Osteoid osteoma.

from a Brodie's abscess, which enhances slower and does not show peak enhancement in the early arterial phase.<sup>13</sup>

### Other Specialized Sequences and “Signs”

#### Chemical Shift MRI

In patients with contraindications to gadolinium contrast, chemical shift MRI may prove beneficial for identifying the nidus.<sup>23</sup> In chemical shift MRI, also known as in-phase/out-

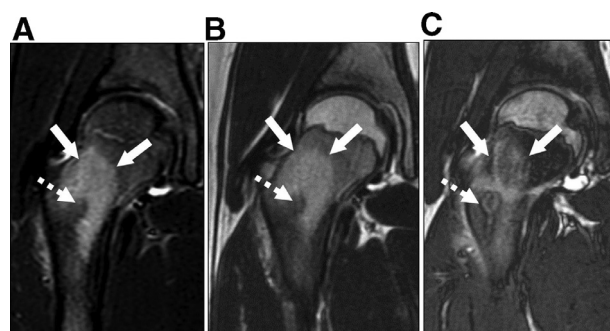


**Figure 6** A 11-year-old girl with chronic right leg pain. Coronal T2-weighted images of the right femur demonstrating an OO lesion (dashed arrows). (A) T2-weighted fat suppressed image showing a low signal OO lesion with surrounding bone marrow edema (solid arrows). Comparing the in-phase (B) and out-of-phase (C) images, the bone marrow edema loses signal on the out-of-phase image because there is fat and fluid in the same voxels. This supports the finding that the surrounding increased signal is bone marrow edema, as opposed to tumor infiltration. The nidus of the OO does not lose signal on the out-of-phase image, supporting the presence of a neoplasm. Combined, these findings should raise suspicion for OO. OO, Osteoid osteoma.

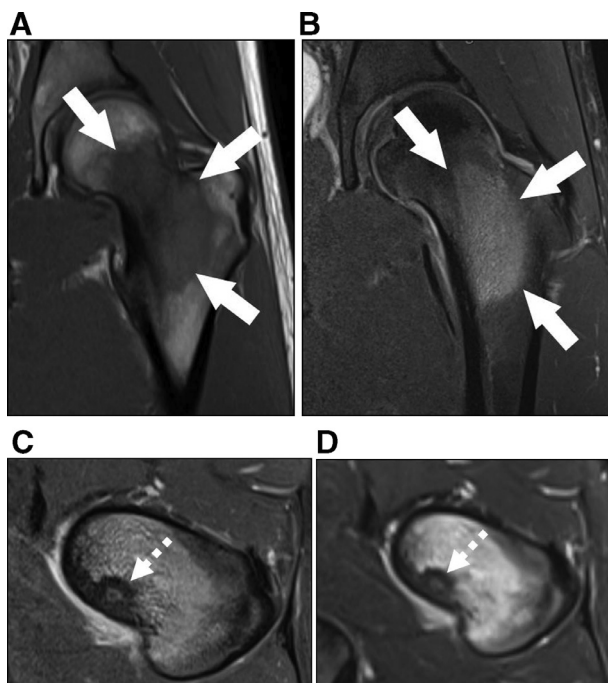


**Figure 7** A 15-year-old boy with severe left hip pain for 3 months. (A) Coronal precontrast T1 and (B) postcontrast T1-weighted fat saturated images demonstrating a half moon sign. This sign manifests on MRI as a semicircular area of bone marrow edema (arrows), with or without a visible nidus, that is located at the femoral neck. Axial (C) T1- and (D) T2-weighted fat saturated images from the same patient displaying a dark rim sign (dashed arrows) representing an area of sclerosis surrounding the nidus.

of-phase imaging, preservation of signal intensity in both phases favors the presence of a neoplasm. Conversely, a relative reduction in signal intensity in the out-of-phase images compared to the in-phase images suggests non-neoplastic tissue. Therefore, OOs have a distinct pattern of signal intensity preservation in both phases at the nidus's location along with a relatively reduced signal intensity in the out-of-phase images in the larger area of surrounding edema (Fig. 6).

### Half Moon Sign

Since femoral and tibial OOs make up the majority of OO lesions, radiologists often have a high index of suspicion for OOs in these bones. However, atypical OOs that are not located in a diaphysis such as in the femoral neck are typically more difficult to detect. It is imperative for clinicians to be able to recognize these types of lesions. In femoral neck lesions, a semicircular area of bone marrow edema in the coronal and axial views can aid in the diagnosis (Fig. 7). Femoral neck OOs are typically endosteal or medullary, which as noted above may be asymmetrically located within surrounding reactive edema thus giving this semicircular or “half-moon” appearance in this location. This finding, known as the “half-moon sign,” was demonstrated by Klontzas et al. to be both sensitive and specific for OO.<sup>24</sup> Their study compared 11 patients with OO to 19 controls that had non-OO causes of proximal femoral bone marrow edema.<sup>24</sup> Shortly after that study was published, Carra et al. published 2 cases

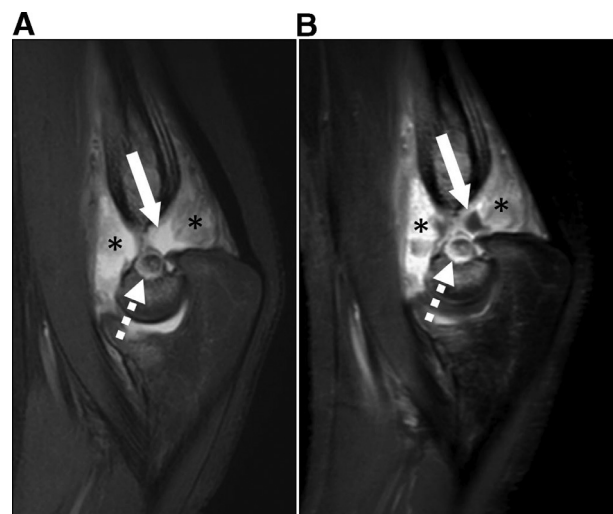


**Figure 8** A 12-year-old girl with chronic elbow pain. An intra-articular, subperiosteal OO in the distal left humerus. Sagittal (A) T2-weighted fat saturated and (B) T1-weighted postcontrast MRIs show a partially calcified nidus (dashed arrows). There is a reactive joint effusion (arrows) with synovial thickening and enhancement (asterisks). OO, Osteoid osteoma.

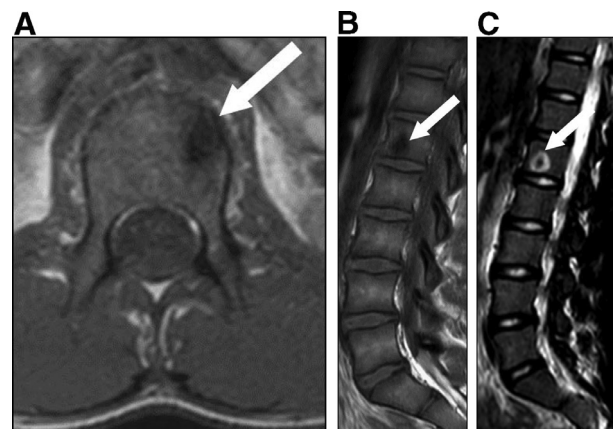


**Figure 9** A 14-year-old girl with persistent low back pain. (A) Axial and (B) sagittal T1-weighted and (C) sagittal T2-weighted fat saturated MRI showing a L1 OO nidus (arrows) with central sclerosis. The peripheral hyperintense signal on T2-weighted images reflects the perilesional marrow edema. OO, Osteoid osteoma.

of stress injury to the femoral neck that challenged the specificity of half-moon sign.<sup>27</sup> They emphasized the importance of considering the history of the patient's pain to rule out stress injuries and suggest proceeding to CT as a next step to locate a potential OO nidus.<sup>27</sup> However, given the findings cited above by Liu et al. and Zama et al. dynamic contrast-enhanced postcontrast imaging would be a more appropriate step in these patients already receiving an MRI.<sup>21,22</sup>

### Dark Rim Sign

Depending on the location of the OO nidus a rim of hypointense signal representing sclerotic tissue may be present (Fig. 7). This is a yet unpublished finding that the authors have noted in multiple OOs. This “dark rim sign” appears as a homogeneously hypointense, thick rim surrounding OO

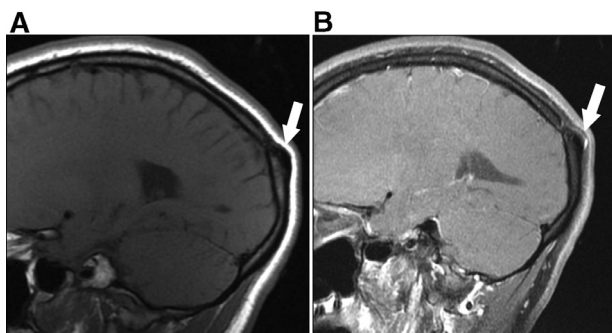


**Figure 10** A 15-year-old girl with a growing lump on the back of her head. (A) Pre- and (B) postcontrast sagittal T1-weighted MRIs show an occipital bone OO (arrows). The nidus is heavily calcified and only a very thin rim of enhancement is seen following contrast administration. OO, Osteoid osteoma.

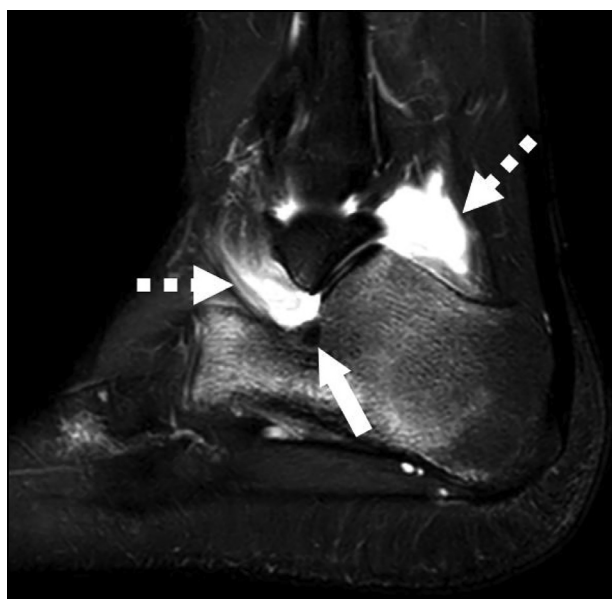


**Figure 11** A 11-year-old girl with chronic left ankle swelling and pain. (A) Sagittal T2-weighted fat saturated image of the left ankle shows a low signal intensity OO lesion (arrows) within the calcaneus with extensive adjacent calcaneal bone marrow edema and reactive subtalar joint effusion (dashed arrows). OO, Osteoid osteoma.

niduses and is a finding that the authors have found to be both specific and sensitive for the diagnosis of OO in endosteal and medullary locations.<sup>28</sup> However, this finding is not typically seen with intracortical OOs. This is because the zone of reactive sclerosis is indistinguishable from the cortical bone in which the nidi of intracortical OOs are embedded.

### Location-Specific Findings

Intra-articular OOs commonly involve the hip but may also involve the ankle, hindfoot, elbow, and other joints. OOs in an intra-articular location typically have minimal, if any, reactive cortical thickening. This is because there is no cambium containing the progenitor cells that develop into osteoblasts in the inner periosteal layer.<sup>25</sup> Intra-articular lesions (Fig. 8) are symptomatically distinct from other types of OO. Patients with these types of lesions complain of arthralgias, stiffness, and swelling due to the reactive joint effusion. This type of lesion is often misdiagnosed since the reactive sclerosis is relatively minimal and the bone marrow edema is more extensive than expected.<sup>29</sup>

Vertebral OOs (Fig. 9) are most often located in the lumbar spine. Depending on what part of the vertebrae is affected, a dark rim sign may or may not be obvious. Vertebral OOs usually affect the posterior elements. Radicular pain and scoliosis are common in patients with vertebral OOs. Indeed OO is one of the causes of painful scoliosis in adolescents, with the scoliotic curve concavity being ipsilateral to the lesion in most cases.<sup>1,30</sup> In rare cases, bones of the skull and mandible can develop OOs (Fig. 10).

Carpal and tarsal lesions are typically medullary and are considered intra-articular when found in these locations. Inflammation usually extends to adjacent joints and nearby bones (Fig. 11). Lesions of the metacarpals, metatarsals, and phalanges are typically intracortical and present with soft tissue swelling, masquerading as infection or arthritis (Fig. 12). Although, painless presentations are not uncommon, particularly involving the phalanges of the hands and feet.<sup>31,32</sup>

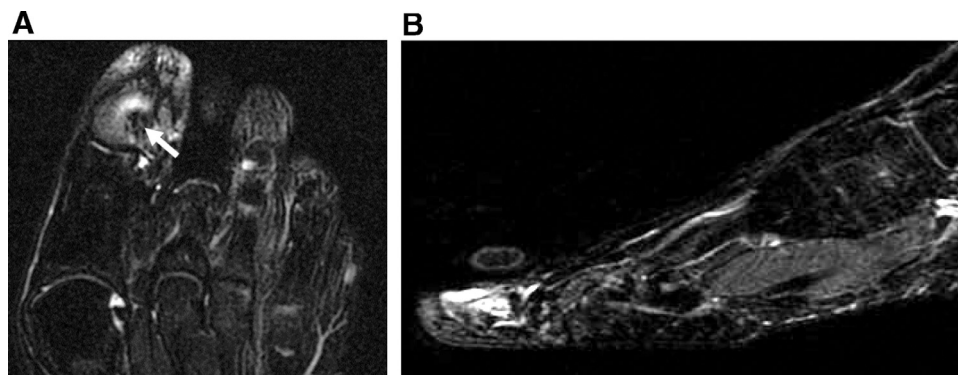


**Figure 12** A 16-year-old girl with chronic left great toe pain. (A) Coronal T2-weighted fat saturated and (B) sagittal STIR images showing bone marrow edema in the distal first phalanx. The nidus (arrow) is seen as low signal intensity on the coronal image (A), which is due to mineralization of the nidus.



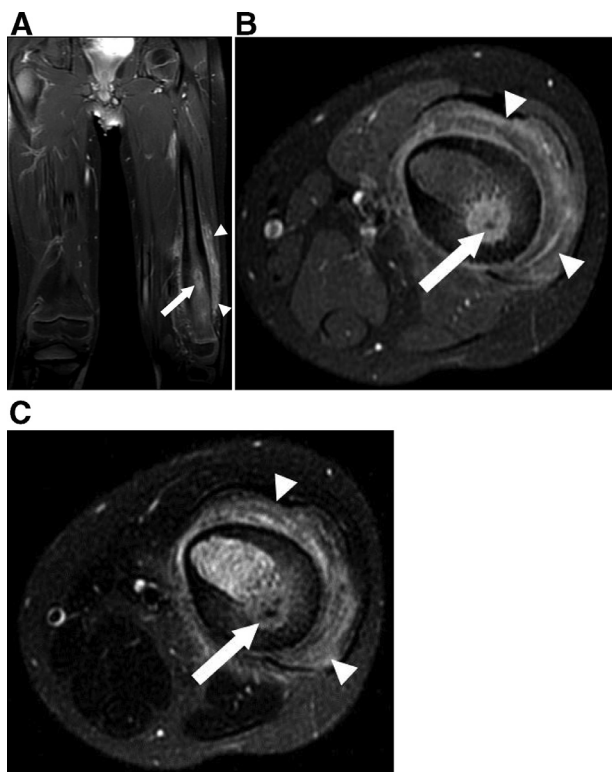


**Figure 13** A 5-year-old boy with a limp and persistent left lower extremity pain that worsens at night and resolves with NSAIDs. (A) Axial and (B) coronal T1-weighted fat saturated postcontrast and (C) axial T2-weighted fat saturated images show the OO nidus (arrows). Surrounding cortical thickening and extensive adjacent inflammatory soft tissue changes can be noted (arrowheads). NSAIDs, nonsteroidal anti-inflammatory drugs; OO, Osteoid osteoma.

## Differential Diagnoses

Osteomyelitis, stress fractures, and other bone neoplasms may resemble OO on imaging and present with clinical findings similar to those seen in patients with OO. Some authors believe that OO has a misleading appearance on MRI that causes the misdiagnosis of infection or a more aggressive lesion.<sup>17-19</sup> It is common to see extensive soft tissue changes in such cases (Fig. 13). Localized tenderness to touch and pressure and local swelling might be present, particularly when the bone involved is in close proximity to the skin.<sup>33</sup> Much of this swelling may be secondary to the highly vascular nature of the tumor, which has been confirmed by angiography, scintigraphy, and Doppler sonography.<sup>34-36</sup> This may also be mediated by the production of prostaglandins, which can affect soft tissue and vascular permeability.<sup>7</sup> Prostaglandins are believed to lead to dilatation and edematous changes of blood vessels in the surrounding medullary tissue, these changes are reflected as hyperintense areas on T2-weighted sequences on MRI.<sup>37,38</sup> This combination of localized swelling and T2-hyperintensity on MRI may be misdiagnosed as infection. Particularly, an intraosseous abscess can mimic the appearance of an OO (Fig. 14). However, an intraosseous abscess should have a rim of enhancement around a central area of necrosis, which does not enhance. In contrast the nidus of an OO typically is vascular and if the nidus of an OO demonstrates the characteristic arterial enhancement pattern, described above (see “Dynamic Contrast Enhanced MRI”), then the OO would be effectively distinguished from osteomyelitis.

A stress fracture is often in the differential diagnosis of OO on radiographs because the cortical thickening may hinder

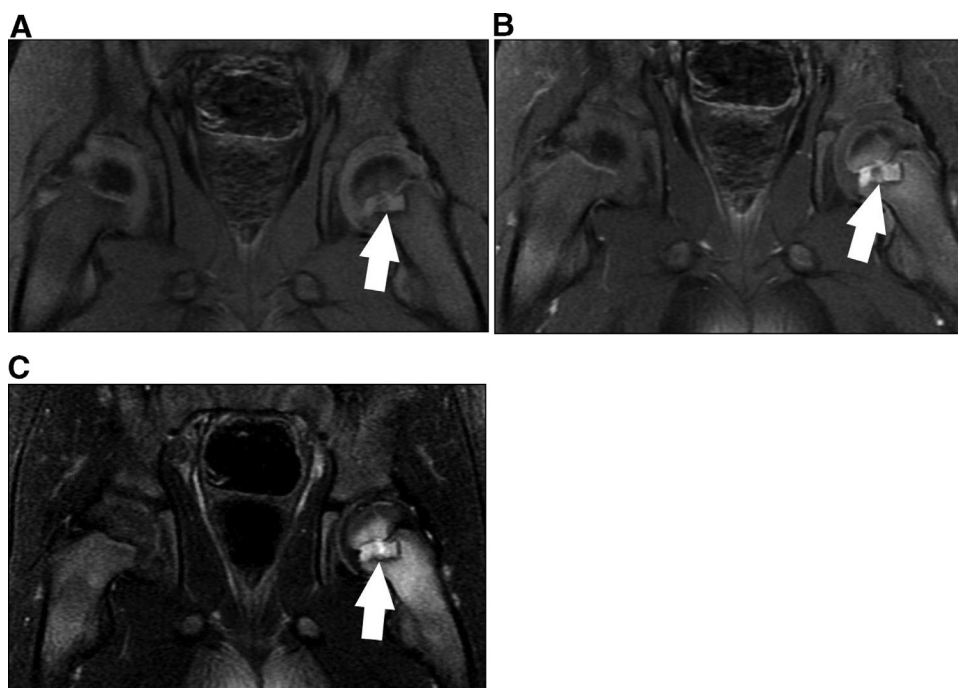


**Figure 14** A 11-year-old boy that presented with limping for three weeks (A) Pre- and (B) postcontrast T1-weighted and (C) T2-weighted fat saturated images. The abscess (arrow) in this case of osteomyelitis could be mistaken for an OO but the thick rim of enhancement surrounding a central area without enhancement on post contrast images and extension across the proximal femoral physis are more characteristic of osteomyelitis with an intraosseous abscess. OO, Osteoid osteoma.



**Figure 15** A 15-year-old male basketball player with chronic right leg pain showing cortical thickening like what is often observed in OO. A linear fracture line (arrowhead) is visible through the anterior tibial cortex. OO, Osteoid osteoma.

detection of a nidus of an OO or the linear fracture line of a stress fracture. On MRI fracture line within an area of cortical thickening will have a different configuration from the nidus of an OO, namely a linear rather than a spherical or ovoid appearance found in OO (Fig. 15). A thorough history can also support a stress fracture over an OO, such as in patients with progressively worsening pain that began after training for a sport or beginning a labor-intensive job.

Other bone neoplasms, such as osteblastomas and chondroblastomas, do not typically display a nidus less than 2 cm with adjacent bone marrow and periosteal edema-like signal, particularly with the characteristic enhancement pattern seen in OO. Osteblastomas, while histologically similar to OO s, are typically larger than 2.5 cm, more commonly involve the spine, have less reactive bone formation and usually appear as expansile lesions. Chondroblastomas can cause abundant adjacent bone marrow and soft tissue edema, but they have a very different imaging appearance — that of a chondroid lesion — with a typical epiphyseal location. As mentioned above, diaphyseal or metaphyseal OOs are much more common than epiphyseal OOs. Langerhans cell histiocytosis can have a varied appearance on imaging as a lytic lesion with either well defined or permeative margins but as with the other lesions mentioned above does not have the focal nidus with surrounding sclerosis and edema that characterize an OO. Primary bone malignancies in children (ie, osteosarcoma and Ewing sarcoma) also have a different imaging appearance from OO with an aggressive poorly defined destructive appearance on radiographs with aggressive periosteal reaction.

It is worth mentioning that untreated OOs can cause growth disturbances that may eventually resemble different

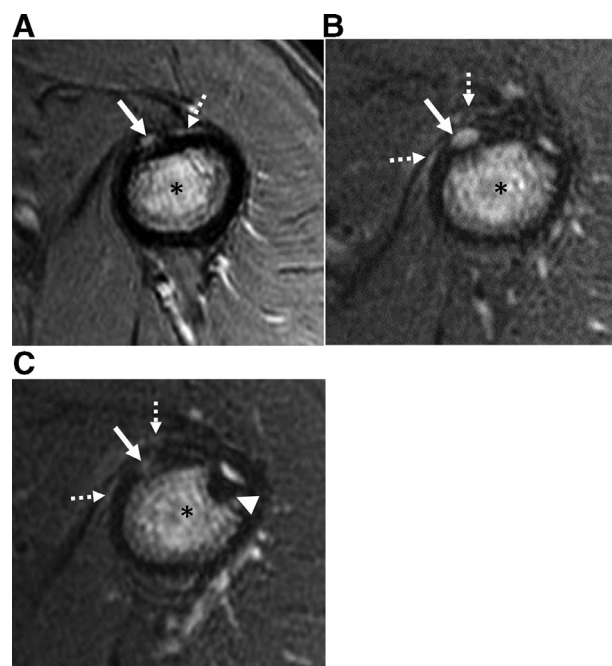


**Figure 16** A 10-year-old boy with left humeral pain. (A) Axial T2-weighted FS MR image at the time of initial presentation shows the nidus (solid arrow) of an OO in the anterior cortex of the proximal humerus. Edema-like signal within the adjacent medullary cavity (asterisk) and periosteal edema-like signal (dashed arrow) are also present. A surgical procedure was performed to resect the OO, however, the pathologic specimen showed reactive bone formation consistent with an OO but the nidus was not present in the resection. (B) and (C) Consecutive axial T2-weighted FS MR images obtained 1 year later because patient had persistent pain. The nidus is increased in size (solid arrows) and adjacent edema-like signal medullary cavity (asterisks) and periosteal soft tissues (dashed arrows) persist. Additionally, the focal area of very low signal intensity (arrowhead in C) represents the resection cavity, which did not include the OO. OO, Osteoid osteoma.

disease processes on MRI and may lead to secondary osseous demineralization from prolonged disuse. A timely and accurate diagnosis is imperative, as the growth disturbances caused by untreated OOs can lead to long-term effects such as abnormal tubulation of long bones, limb length discrepancy, joint contractures, or scoliosis.

## Treatment and Post-treatment MRI

OOs may occasionally be amenable to conservative management if symptoms are mild and well-managed with anti-inflammatory medications. Resolution of symptoms is not common, and if they resolve, many months of medication may be required. Therefore, conservatively managed patients typically have to tolerate the long-term use of anti-inflammatory medications and their potential complications. Removal or ablation of the nidus remains the most effective treatment for the majority of patients and often provides immediate relief. Minimally invasive imaging-guided ablation techniques have become the preferred method for treatment, as they are less destructive to the bone than open surgery and



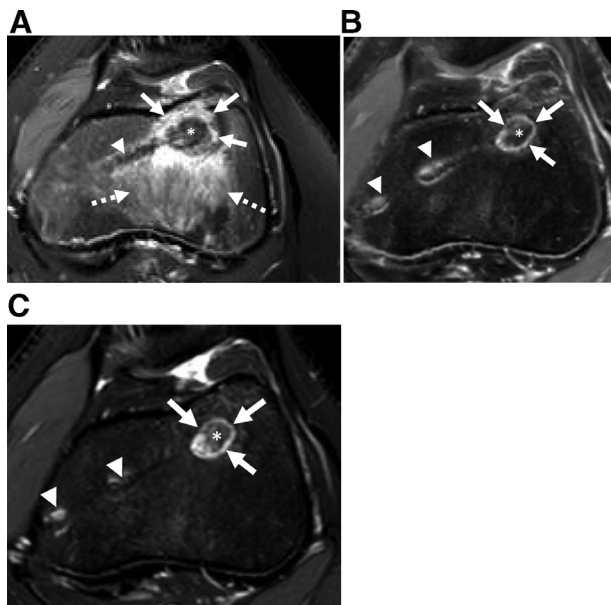


**Figure 17** A 14-year-old girl with a distal femoral osteoid osteoma, status post radiofrequency ablation. (A) Axial T2-weighted fat saturated MR image performed one week after ablation procedure. An expected “target” appearance is seen at the ablation site. Centrally there is low signal (asterisk), at the tip of the tract from the ablation probe (arrowhead), which has been termed zone 1 (Z1). Zone 2 (Z2) is a well-defined rim of increased signal intensity (solid arrows) immediately peripheral to and surrounding Z1. Zone 3 (Z3) is the less well-defined area of edema-like signal peripheral to Z2 (dashed arrows). (B) Axial T2-weighted and (C) axial T1-weighted post-contrast fat saturated MR images performed 3 months after the ablation procedure. There has been interval contraction of Z2 (solid arrows), which shows a persistent rim of increased signal on the T2-weighted image and enhancement on the postcontrast image around Z1 (asterisk). Also the edema-like signal previously seen in Z3 has nearly resolved. The ablation tract is noted (arrowheads).

allow for a more expedient recovery. Open surgery is necessary in certain situations. Particularly, in cases where neurovascular or other structures limit the accessibility of the lesion with minimally invasive percutaneous approaches. Additionally, surgery may be necessary for atypical OOs when CT-guided biopsy of the lesion is nondiagnostic and more tissue is needed. Open surgery is also preferred for intra-articular lesions to minimize the possibility of iatrogenic injury to the articular cartilage.

Resolution of clinical symptoms is the typical measure of treatment success. When surgical treatment is performed pathology can define whether there has been a complete or incomplete resection of the nidus. However, pathologic confirmation of complete treatment is not possible with percutaneous ablative procedures. In cases of incomplete resection or incomplete ablation MRI can be helpful to show residual OO (Fig. 16). Some researchers have reported the postablative appearance of OO on MRI.<sup>39-42</sup> One such paper described a target-like postablation appearance on MRI, which becomes apparent 1 week to 2 months after the treatment<sup>40</sup> (Fig. 17). This target-like area contains 3 zones. A

central ablated zone (Z1) that is nonenhancing and is hypointense on T1- and T2-weighted sequences. Surrounding Z1 is a band (Z2) of peripheral enhancement and hyperintensity on T2-weighted sequences. Peripheral to Z2 is a less well-defined area of mild enhancement and hyperintense T2-weighted signal which gradually fades into the adjacent normal tissue.<sup>40</sup> On subsequent follow-up exams these authors noted interval contraction and inward progression of Z2 enhancement; as this evolution continued the distinction between Z1 and Z2 becoming indiscernible as both diminished in size.<sup>40</sup> Concomitantly, the abnormal signal and enhancement in Z3 gradually fades. If in contrast to that normal postablative appearance, if there is persistence of a nidus with peak arterial enhancement on dynamic MRI, then recurrent or residual OO is likely present.<sup>13</sup>

## Conclusion

It is important for radiologists to familiarize themselves with the many appearances of OO on MRI. Realizing that the different types of OO (subperiosteal, cortical, endosteal, or medullary) can have different imaging appearances and OOs in locations outside the diaphysis of long bones also can have atypical appearances. Older literature has suggested that CT has increased sensitivity and specificity, compared to MRI, for diagnosing OO. However, more recent studies utilizing dynamic contrast-enhanced MR sequences have challenged that notion. Additionally, children who present with OOs in atypical locations, such as intra-articular lesions, will typically proceed to MRI if the diagnosis is not made on radiographs. By utilizing dynamic postcontrast images and other sequences and signs reviewed here, radiologists should be able to diagnose the majority of OOs on MRI with a high level of confidence.

## References

1. Kransdorf MJ, Stull MA, Gilkey FW, et al: Osteoid osteoma. *Radiographics* 11:671-696, 1991. <https://doi.org/10.1148/radiographics.11.4.1887121>
2. White LM, Kandel R: Osteoid-producing tumors of bone. *Semin Musculoskelet Radiol* 4:25-43, 2000. <https://doi.org/10.1055/s-2000-6853>
3. Czerniak B: Dorfman and Czerniak's Bone Tumors. (4th edn.). Philadelphia, PA: Elsevier, 2016
4. Greenspan A, Jundt G, Remagen W: Bone-forming (Osteogenic) lesions. *Differential Diagnosis in Orthopaedic Imaging*. Philadelphia: Lippincott Williams and Wilkins, 40-159, 2007
5. Healey JH, Ghelman B: Osteoid osteoma and osteoblastoma. *Current concepts and recent advances*. *Clin Orthop Relat Res*: 76-85, 1986
6. Greco F, Tamburrelli F, Ciabattini G: Prostaglandins in osteoid osteoma. *Int Orthop* 15:35-37, 1991. <https://doi.org/10.1007/bf00210531>
7. Mungo DV, Zhang X, O'Keefe RJ, et al: COX-1 and COX-2 expression in osteoid osteomas. *J Orthop Res* 20:159-162, 2002. [https://doi.org/10.1016/s0736-0266\(01\)00065-1](https://doi.org/10.1016/s0736-0266(01)00065-1)
8. Kneisl JS, Simon MA: Medical management compared with operative treatment for osteoid-osteoma. *J Bone Joint Surg Am* 74:179-185, 1992
9. Koch G, Cazzato RL, Gilkison A, et al: Percutaneous treatments of benign bone tumors. *Semin Intervent Radiol* 35:324-332, 2018. <https://doi.org/10.1055/s-0038-1673640>

10. Neyisci C, Erdem Y: Safe and effective treatment choice for osteoid osteoma: Computed tomography-guided percutaneous radiofrequency ablation. *Cureus* 11:e5526, 2019. <https://doi.org/10.7759/cureus.5526>
11. Yu X, Wang B, Yang S, et al: Percutaneous radiofrequency ablation versus open surgical resection for spinal osteoid osteoma. *Spine J* 19:509-515, 2019. <https://doi.org/10.1016/j.spinee.2018.07.013>
12. Kayser F, Resnick D, Haghighi P, et al: Evidence of the subperiosteal origin of osteoid osteomas in tubular bones: Analysis by CT and MR imaging. *AJR Am J Roentgenol* 170:609-614, 1998. <https://doi.org/10.2214/ajr.170.3.9490939>
13. Pottecher P, Sibilleau E, Aho S, et al: Dynamic contrast-enhanced MR imaging in osteoid osteoma: Relationships with clinical and CT characteristics. *Skeletal Radiology* 46:935-948, 2017. <https://doi.org/10.1007/s00256-017-2645-2>
14. Spouge AR, Thain LM: Osteoid osteoma: MR imaging revisited. *Clin Imaging* 24:19-27, 2000
15. Klein MH, Shankman S: Osteoid osteoma: Radiologic and pathologic correlation. *Skeletal Radiol* 21:23-31, 1992. <https://doi.org/10.1007/bf00243089>
16. Assoun J, Richardi G, Railhac JJ, et al: Osteoid osteoma: MR imaging versus CT. *Radiology* 191:217-223, 1994. <https://doi.org/10.1148/radiology.191.1.8134575>
17. Davies M, Cassar-Pullicino VN, Davies AM, et al: The diagnostic accuracy of MR imaging in osteoid osteoma. *Skeletal Radiol* 31:559-569, 2002. <https://doi.org/10.1007/s00256-002-0546-4>
18. Goldman AB, Schneider R, Pavlov H: Osteoid osteomas of the femoral neck: Report of four cases evaluated with isotopic bone scanning, CT, and MR imaging. *Radiology* 186:227-232, 1993. <https://doi.org/10.1148/radiology.186.1.8416569>
19. Hosalkar HS, Garg S, Moroz L, et al: The diagnostic accuracy of MRI versus CT imaging for osteoid osteoma in children. *Clin Orthop Relat Res*: 171-177, 2005
20. Zanetti M, Eberhard SM, Exner GU, et al: Magnetic resonance tomography in osteoid osteoma: More confusion than benefit? *Praxis (Bern 1994)* 86:432-436, 1997
21. Liu PT, Chivers FS, Roberts CC, et al: Imaging of osteoid osteoma with dynamic gadolinium-enhanced MR imaging. *Radiology* 227:691-700, 2003. <https://doi.org/10.1148/radiol.2273020111>
22. Zampa V, Bargellini I, Ortori S, et al: Osteoid osteoma in atypical locations: The added value of dynamic gadolinium-enhanced MR imaging. *Eur J Radiol* 71:527-535, 2009. <https://doi.org/10.1016/j.ejrad.2008.05.010>
23. Costa FM, Canella C, Vieira FG, et al: The usefulness of chemical-shift magnetic resonance imaging for the evaluation of osteoid osteoma. *Radiol Bras* 51:156-161, 2018. <https://doi.org/10.1590/0100-3984.2017.0037>
24. Klontzas ME, Zibis AH, Karantanas AH: Osteoid osteoma of the femoral neck: Use of the half-moon sign in MRI diagnosis. *AJR Am J Roentgenol* 205:353-357, 2015. <https://doi.org/10.2214/ajr.14.13689>
25. Chai JW, Hong SH, Choi JY, et al: Radiologic diagnosis of osteoid osteoma: From simple to challenging findings. *Radiographics* 30:737-749, 2010. <https://doi.org/10.1148/rg.303095120>
26. Teixeira PA, Chanson A, Beaumont M, et al: Dynamic MR imaging of osteoid osteomas: correlation of semiquantitative and quantitative perfusion parameters with patient symptoms and treatment outcome. *Eur Radiol* 23:2602-2611, 2013. <https://doi.org/10.1007/s00330-013-2867-1>
27. Carra BJ, Chen DC, Bui-Mansfield LT: The half-moon sign of the femoral neck is nonspecific for the diagnosis of osteoid osteoma. *AJR Am J Roentgenol* 206. <https://doi.org/10.2214/AJR.15.15610>, 2016. W54-W54
28. French J, Epelman M, Kraus M, et al: MRI Findings in Osteoid Osteoma. In: 104th Scientific Assembly and Annual Meeting; Radiological Society of North America (RSNA), Chicago, IL, 2019; Chicago, IL. Nov 25-30
29. Gaeta M, Minutoli F, Pandolfo I, et al: Magnetic resonance imaging findings of osteoid osteoma of the proximal femur. *Eur Radiol* 14:1582-1589, 2004. <https://doi.org/10.1007/s00330-004-2293-5>
30. Lefton DR, Torrisi JM, Haller JO: Vertebral osteoid osteoma masquerading as a malignant bone or soft-tissue tumor on MRI. *Pediatr Radiol* 31:72-75, 2001. <https://doi.org/10.1007/s002470000378>
31. Basu S, Basu P, Dowell JK: Painless osteoid osteoma in a metacarpal. *J Hand Surg Br* 24:133-134, 1999. <https://doi.org/10.1054/jhsb.1998.0048>
32. Ekmekci P, Bostanci S, Erdogan N, et al: A painless subungual osteoid osteoma. *Dermatol Surg* 27:764-765, 2001. <https://doi.org/10.1046/j.1524-4725.2001.00332.x>
33. Swee RG, McLeod RA, Beabout JW: Osteoid osteoma. Detection, diagnosis, and localization. *Radiology* 130:117-123, 1979. <https://doi.org/10.1148/130.1.117>
34. Gil S, Marco SF, Arenas J, et al: Doppler duplex color localization of osteoid osteomas. *Skeletal Radiology* 28:107-110, 1999. <https://doi.org/10.1007/s002560050484>
35. Helms CA, Hattner RS, Vogler JB 3rd: Osteoid osteoma: Radionuclide diagnosis. *Radiology* 151:779-784, 1984. <https://doi.org/10.1148/radiology.151.3.6232642>
36. Lindbom Å, Lindvall N, Soderberg G, et al: Angiography in osteoid osteoma. *Acta Radiol* 54:327-333, 1960. <https://doi.org/10.3109/00016926009172555>
37. Kawaguchi Y, Hasegawa T, Oka S, et al: Mechanism of intramedullary high intensity area on T2-weighted magnetic resonance imaging in osteoid osteoma: A possible role of COX-2 expression. *Pathol Int* 51:933-937, 2001. <https://doi.org/10.1046/j.1440-1827.2001.01305.x>
38. Yamamura S, Sato K, Sugiura H, et al: Prostaglandin levels of primary bone tumor tissues correlate with peritumoral edema demonstrated by magnetic resonance imaging. *Cancer* 79:255-261, 1997
39. Cantwell CP, Kerr J, O'Byrne J, et al: MRI features after radiofrequency ablation of osteoid osteoma with cooled probes and impedance-control energy delivery. *AJR Am J Roentgenol* 186:1220-1227, 2006. <https://doi.org/10.2214/ajr.05.0149>
40. Lee MH, Ahn JM, Chung HW, et al: Osteoid osteoma treated with percutaneous radiofrequency ablation: MR imaging follow-up. *Eur J Radiol* 64:309-314, 2007. <https://doi.org/10.1016/j.ejrad.2007.06.023>
41. Mahnken AH, Bruners P, Delbruck H, et al: Contrast-enhanced MRI predicts local recurrence of osteoid osteoma after radiofrequency ablation. *J Med Imaging Radiat Oncol* 56:617-621, 2012. <https://doi.org/10.1111/j.1754-9485.2012.02443.x>
42. Vanderschueren GM, Taminiau AH, Obermann WR, et al: The healing pattern of osteoid osteomas on computed tomography and magnetic resonance imaging after thermocoagulation. *Skeletal Radiol* 36:813-821, 2007. <https://doi.org/10.1007/s00256-007-0319-1>